J. Membrane Biol. 8, 389–402 (1972)

Transport Phenomena in a Model Membrane Accompanying a Conformational Change: Membrane Potential and Ion Permeability

Mizuko Yoshida*, Naoki Kamo, and Yonosuke Kobatake

Faculty of Pharmaceutical Sciences, Hokkaido University, Sapporo, Japan, 060

Received 1 November 1971

Summary. Membrane potential $\Delta\varphi_m$ ion permeability P and d-c conductance G_p^0 of a model membrane composed of a filter paper and a synthetic lipid analogue, i.e. dioleylphosphate (DOPH), were observed in various concentrations of 1:1 type electrolyte solution. With successive increases of salt concentration in the external solution, $\Delta\varphi_m$, P and G_p^0 changed their values rather discontinuously at a certain critical value of the concentration c_t. When the concentration was decreased successively, the values of $\Delta\varphi_m$, P and G_p^0 were returned to the original levels at a concentration much lower than c_t. Thus, the transport phenomena observed across the membrane showed an appreciable hysteresis loop.

The discontinuous variations of $\Delta\varphi_m$, P and G_p^0 were interpreted in terms of a transition of DOPH adsorbed in the filter paper from an oil membrane to a charged membrane. This transformation of DOPH at the critical salt concentration is consistent with the previous argument that the DOPH impregnated in the filter paper changes its conformation from oil droplets to a number of bilayer films, which deduced from a theoretical analysis of frequency dependency of the electrical capacitance of the membrane.

Recent electrochemical studies on squid giant axons suggest that the process of excitation of nervous tissues is accompanied by a conformational change of the macromolecules constituting the membrane, triggered by cooperative cation exchange at fixed negative sites in the membrane [3, 7, 8, 9]. Changes in thermal and optical properties of nervous tissues during excitation support this argument [1, 2]. There is serious ambiguity, however in interpreting the results of physical measurements carried out on nerves, since there are many undefinable quantities in a system consisting of an excitable membrane and its natural environment, and since the molecular

* *Permanent address:* Tokyo Institute of Technology, Meguro, Tokyo, Japan.

structures and their conformation of the living membrane are not entirely known up to the present. Therefore, it is necessary to study, as a counterpart of investigations on living tissues, the transport processes in a model system in which a definite transformation of the molecular conformation in the membrane takes place with the variation of the environmental salt condition, or with an external stimulus. In other words, the correlation between the transmembrane phenomena and the state of the membrane must be clarified with a well-defined physico-chemical system. Studies described in this series of papers have been undertaken along this line of thought. A similar attempt was discussed by Tobias, Agin and Pawlowski [10] some years ago.

In a different series of papers [5, 12] concerned with the electrical capacitance of membranes, we described a characteristic behavior of impedance in a model membrane composed of a filter paper and a synthetic lipid analogue, i.e. dioleylphosphate (DOPH). Thus, the electric capacitance and conductance of the membrane changed discontinuously with successive increase of the external concentration of a 1:1 type electrolyte, when the salt concentration reached to a certain critical value c_t. The critical concentration c_t depended on the adsorbed quantity of DOPH for a given pore size ϕ of the filter paper used as a substrate.

This paper describes the experimental studies of the steady transport processes of the membrane composed of a filter paper and DOPH. The membrane potential, ion permeability, and d-c conductance of the membrane are measured as a function of the external salt concentration, with a view to obtaining more secure information about the transformation of DOPH impregnated in the filter paper. The results may be interpreted in terms of the theoretical membrane model proposed in the previous articles [5, 12]. Subsequent papers will be concerned with transient processes in response to external stimuli in the same membrane system, anticipating that the physico-chemical analysis of the model membrane put forward in this series may have some value for better understanding of the molecular mechanism of the excitation of living membranes.

Materials and Methods

The dioleylphosphate (DOPH) used as a lipid analogue was the same as that used in the previous studies [5, 12]. The millipore filter paper composed of cellulose ester of nominal pore size 5 μm and thickness of 0.1 mm was soaked about a half-hour in a benzene solution of DOPH at a given concentration, with which the adsorbed quantity of DOPH in the filter paper was adjusted. In the present study, we confined ourselves to the case where the adsorbed quantity of DOPH in the filter paper was fixed approxi-

mately at 2.0 mg/cm^2, since the membrane at this condition exhibited the clearest discrete variation in the observed electrical capacitance C_p at the critical concentration with successive increase of the external KCl or NaCl concentration [12]. With this condition, c_t was about 30 to 40 mM. The soaked filter paper was dried in the air. The amount of DOPH adsorbed in the filter paper Q (mg/cm^2) was determined by weighing. The filter paper containing DOPH was immersed and conditioned overnight in an aqueous solution of KCl or NaCl of 1/8 M, and used as the sample membrane. The KCl was purified by repeated crystallization, and NaCl of analytical grade was used as delivered. The water used as solvent was prepared by treating distilled water with both cation and anion exchangers. The pH of the water was 5.5 throughout the present study.

Measurements of Impedance and Membrane Potential

The cell, apparatus, and procedures for the measurements of the membrane impedance were essentially the same as those reported in the previous paper [5]. A pair of Pt-Pt plate electrodes, 1 cm^2 in area, was placed as close to the membrane as possible. The applied frequency ν was changed between 20 Hz and 3 MHz.

Fig. 1 shows a schematic diagram of the cell used for measuring membrane potential and ion permeability. The emf in two sides of the membrane was conducted to a vibrating reed electrometer (Takeda Riken Co., Type TR-84B) through two Ag-AgCl electrodes, and recorded in a pen recorder when necessary. The asymmetry potential of the two Ag-AgCl electrodes was less than 0.1 mV in the whole range of salt concentration studied. The Ag-AgCl electrodes were replaced by a pair of Pt-Pt electrodes, 1 cm^2 in area, when the impedance was observed under the same external condition with that for the emf measurements. The emf between two electrodes with no membrane was subtracted from the measured emf to obtain the desired membrane potential $\Delta\varphi_m$. The measurements were repeated two or three times at a given condition, and their averaged value was taken as a data point of $\Delta\varphi_m$. The bulk solutions were stirred vigorously by a pair of magnetic stirrers. The ratio of concentrations in two sides of the membrane $\beta = C_2/C_1$ was fixed at 2.0 or 4.0 in a series of experiments unless otherwise noted. The concentrations were varied successively from 1/1024 to 1/4 moles/liter (M).

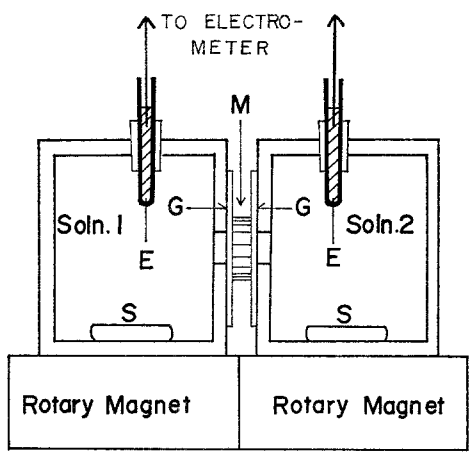

Fig. 1. Schematic diagram of the cell used for measurements of membrane potential and ion flux. *E* Electrode; *M* membrane; *G* gasket; *S* stirrer tip

Measurements of Ion Fluxes

The flux of Na^+ ions across the membrane was measured by use of Na^{22} in a given concentration of NaCl solution. The radioactive tracer was added into the solution in the one compartment of the cell shown in Fig. 1, and the radioactivity appearing in the other compartment (cold compartment, the initial volume of which was 40.0 ml) was determined at time intervals between 5 min and 1 hr. The volume of the radioactive sample taken from the cold or hot compartment was 1.0 ml, and the radioactivity of an individual sample was measured by a liquid scintillation spectrometer (Beckmann, Type CMP-100). The decrement of the liquid volume in the cold compartment caused by sampling was corrected by calculation each time. After a delay, which was less than 30 min in most of the present measurements, the radioactivity in the cold compartment rose linearly with time. The flux of ions is determined from the slope of the linear rise in the radioactivity in the cold compartment, and the permeability of Na^{22} across the membrane can be defined by $P=(\text{CPM sec}^{-1})(A/LV)^{-1}c^{*-1}$. Here A and L are the effective area and thickness of the membrane, V is the volume of the cold compartment, and c^* is the radioactivity in the hot compartment in CPM cm^{-3}, which was not varied during one series of measurements. Neither electrical potential nor hydrostatic pressure difference was applied externally to the membrane during the flux measurements. The bulk solutions were stirred vigorously as in the case of the membrane potential measurements.

All observations described above were carried out in an air oven regulated at 25 °C.

Results and Discussion

Impedance of the Membrane

Since the frequency dependence of the electrical capacitance and conductance of the Millipore-DOPH membrane with variety of c_s and Q were discussed precisely in the previous papers [5, 12], only the relevant results are referred to in this article. Fig. 2 shows the capacitance of the membrane C_p as a function of the reduced frequency $\omega\tau$ in various salt concentrations for the system of $\phi=5$ μm with $Q=2.20$ mg/cm^2 in KCl solution. It was noted that KCl and NaCl gave no difference for the impedance of the membrane. In Fig. 2, ω is the applied angular frequency defined by $\omega=2\pi\nu$, and τ is the relaxation time of a DOPH bilayer film in an electrolyte solution of a given concentration, and defined by $\tau=CR_0$. Here C is the electric capacitance of unit area of DOPH bilayer film and equal to 0.35 μF/cm^2, and R_0 is the d-c resistance of a membrane with no DOPH, which is inversely proportional to the salt concentration c_s. It is seen that the electric capacitance of the membrane in various c_s can be divided into two groups at a critical salt concentration c_t, i.e. a group in a dilute salt solution between 1 mM and 30 mM in c_s, and that in a concentrated solution higher than 40 mM. C_p in the low frequency limit, denoted by C_p^0, in these two groups differ from each other more than a factor of ten. We refer to these two

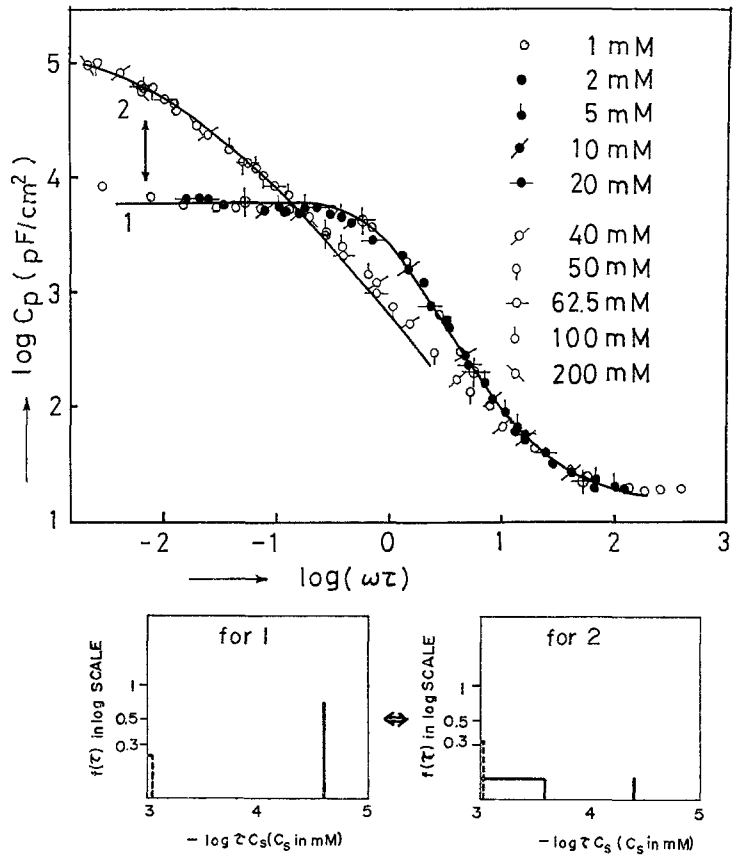

Fig. 2. Electric capacitance C_p of a Millipore-DOPH membrane in various KCl concentrations, as a function of the reduced angular frequency $\omega\tau$. $Q=2.20$ mg/cm². *Bottom left:* the distribution function of the relaxation time $f(\tau)$ plotted against τc_s both in logarithmic scale for curve *1*; *Bottom right:* $\log f(\tau)$ *vs.* $-\log(\tau c_s)$ relation for curve *2*, with c_s in mM

groups as groups *1* and *2*, respectively, as noted in Fig. 2. It was noted in the previous paper that the frequency dependence of curve *1* was represented quantitatively by a single dispersion, and hence a δ-function for the distribution function of τ was enough to reproduce the frequency dispersion of C_p. On the other hand, curve *2* was represented in terms of two distinct distribution functions of τ, i.e. one δ-function and one box type distribution as shown in the bottom of the figure, where the distribution function $f(\tau)$ is plotted against τc_s for curves *1* and *2*. The box type distribution of large τ stemmed from a number of bilayer leaflets of DOPH formed in the void space of the Millipore filter paper [12]. From these theoretical results, it was inferred that the DOPH in the filter paper changes its confor-

mation from oil droplets in a dilute solution to a number of bilayer films in a concentrated solution at the critical salt concentration c_t. We would not argue that the mechanism described above is the sole cause of the discrete variation of C_p. It must be one of many others which may account equally well for experimental facts. However, the actual mechanism occurring in the membrane is not immaterial for the subsequent arguments, since the present paper intends to clarify the correlation between the membrane phenomena and the state of membrane matrix, and to know how the transformation of the membrane matrix is reflected to the transmembrane phenomena.

Ion Permeability and Conductance of the Membrane

The conformational change of DOPH described above can be confirmed by experiments on the ion permeability and on the electrical conductance. Fig. 3 shows the flux of Na^{22} in CPM/cm^2 as a function of time in various NaCl concentrations in the external solution. The membrane used in this study was $Q=2.14$ mg/cm^2. As seen in the figure, the isotope flux was practically zero when the concentration of NaCl was less than 1/128 M. When c_s was raised to 1/64 M, the Na^{22} flux increased gradually with time during approximately three hours. After this induction period, the radioactivity in the cold compartment increased linearly with time. Thus the permeability of Na^{22} given by the slope of this plot became a constant at this stage. When the NaCl concentration rose to 1/32 M or more, the permeability of Na^{22} was not altered by an increase of c_s. If the concentration of NaCl was decreased from 1/8 M, the permeability of the isotopes was not changed appreciably within a few hours, even when c_s was lower than c_t. This was observed until c_s was decreased as low as 1 mM, unless the membrane was allowed to stand in a dilute solution more than several hours. Fig. 4 shows the relative values of ion permeability of the Millipore-DOPH membrane P/P_0 as a function of the external NaCl concentration c_s. Here P_0 is the permeability of Na^{22} in a Millipore filter alone containing no DOPH, and given by the equation: $P_0=(RT/F)u_0$, where u_0 is the mobility of the Na^+ ion in the free solution, and R, T and F have their usual thermodynamic meanings. P_0 is also evaluated experimentally by use of an isotope flux. As seen in the figure, P/P_0 are practically zero in a dilute NaCl solution, and increased rather discontinuously at 1/64 M of c_s, and remained at the same value with further increase of c_s. When c_s was decreased, this value of P/P_0 stayed approximately constant in a dilute solution whose concentration was much lower than 1/64 M. Thus, the permeability of Na^{22} in the

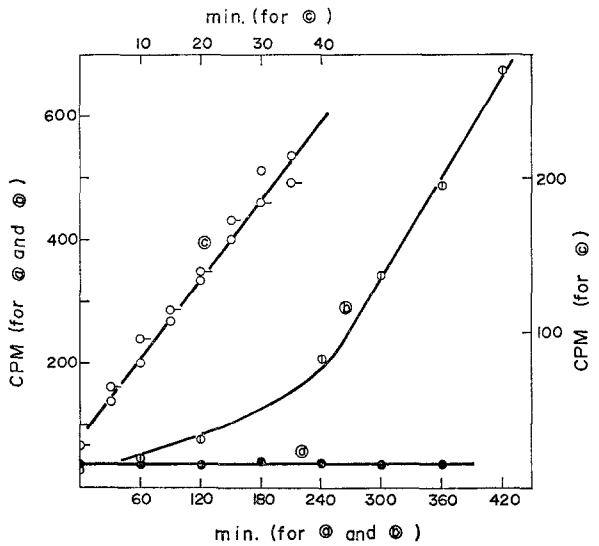

Fig. 3. Na^{22} flux as a function of time for a membrane with $Q=2.14$ mg/cm^2 in various NaCl concentrations. ● 1/128 M NaCl; ⊕ 1/64 M NaCl; ○ 1/32 M NaCl; ○- 1/16 M NaCl

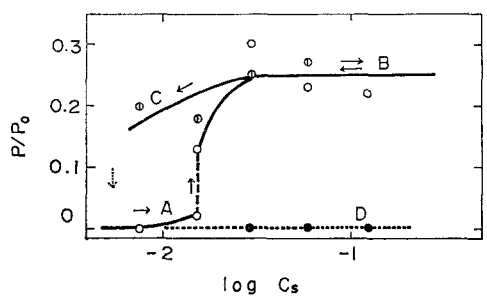

Fig. 4. The reduced permeability of Na^{22} P/P_0 plotted against logarithm of NaCl concentration c_s. The system is the same as in Fig. 3. ○ Successive increase of c_s; ⊕ successive decrease of c_s

Millipore-DOPH membrane showed an appreciable hysteresis loop as illustrated by arrows in the figure. Another membrane with different Q showed the similar hysteresis curve for P/P_0 when c_s was changed successively, although the critical salt concentration c_t at which P/P_0 increased discontinuously depended upon the value of Q. For example, in a membrane with $Q=5.0$ mg/cm^2 no permeation of radioisotope was observed in the whole range of the external salt concentration studied. For the purpose of comparison, this was also plotted in Fig. 4, and connected by a dotted

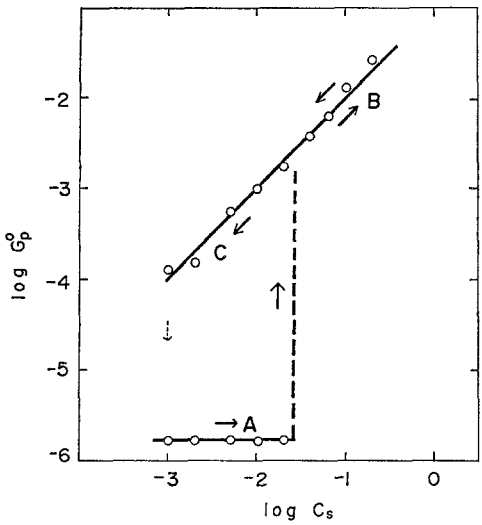

Fig. 5. d-c conductance of a membrane G_p^0 as a function of KCl concentration c_s. The system is the same as in Fig. 2. The KCl concentration is changed successively following arrows

line. For convenience of illustration, four different segments in P/P_0 *vs.* log c_s plots shown in Fig. 4 are designated as *A*, *B*, *C*, and *D* as noted in the figure.

Similarly, Fig. 5 shows the d-c conductance of the Millipore-DOPH membrane in various KCl concentrations. In a dilute salt solution, the conductance is independent of the external salt concentration with a very small value of G_p^0, the order of magnitude of G_p^0 being 1 μmho cm^{-2}. When c_s reached to the critical concentration c_t, G_p^0 increased discontinuously by about a factor of 10^3, and after that G_p^0 increased with c_s. When c_s was decreased from this stage, G_p^0 decreased with c_s almost linearly until c_s attained as low as only a few mM. With sufficient conditioning of the membrane in a few mM KCl solution, the value of G_p^0 decreased to the original value, and repeated the same cycle with the successive variation of c_s as illustrated by arrows in Fig. 5.

Membrane Potential

Fig. 6 shows the discrete variation and the hysteresis of the membrane potential $\Delta\varphi_m$ of the Millipore-DOPH membrane with $Q=1.49$ mg/cm^2 in NaCl solution, where $\Delta\varphi_m$ is plotted against log C_2. Here the concentration of NaCl in one side of the membrane (C_1) was fixed at 1/256 M, and that in the other compartment changed successively. When C_2 was lower than

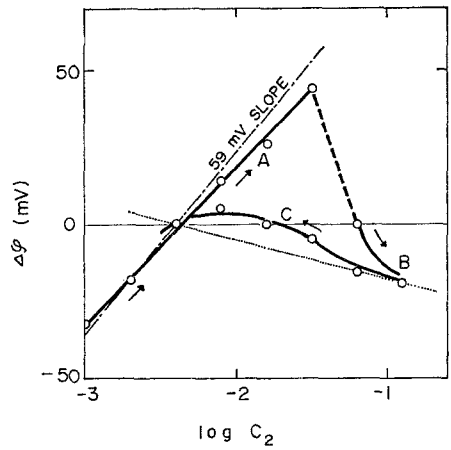

Fig. 6. Membrane potential data $\Delta\varphi_m$ as a function of log C_2 for a membrane with $Q=1.49$ mg/cm^2 in NaCl solution. C_1 is fixed at 1/256 M, and C_2 is changed successively following arrows. -·-·-· Theoretical value of $\Delta\varphi_m$ for an ideal permselective negative membrane; ···· theoretical diffusion potential of NaCl in the free solution

c_t (1/16 M for this specific membrane), the slope of $\Delta\varphi_m$ *vs.* log C_2 plot gave approximately the ideal value of 59 mV per 10-fold variation of C_2. However, when C_2 arrived at c_t, $\Delta\varphi_m$ became about zero. Further increase of C_2 led a negative $\Delta\varphi_m$ (curve *B*), i.e. the concentrated side became positive. The decrease of C_2 from this stage led a gradual increase of $\Delta\varphi_m$ as illustrated by arrow *C*. It is noted that the concentration dependence of curves *B* and *C* is not very different from that for the diffusion potential of NaCl in the bulk solution, i.e. $\Delta\varphi_m=(RT/F)(1-2\,\tau^0_-)\ln(C_2/C_1)$, which is shown by a dotted line in Fig. 6. Here τ^0_- is the transference number of anion in the bulk solution of NaCl. Slight deviation of the observed $\Delta\varphi_m$ from the dotted line stems from the charges fixed on the membrane.

Fig. 7 shows another manifestation of the discrete variation of the membrane potential for a Millipore-DOPH membrane with $Q=2.0$ mg/cm^2 in various KCl concentrations, where the ratio of concentrations in two sides of the membrane $\beta=C_2/C_1$ was fixed at 2.0. The measurement of $\Delta\varphi_m$ was started from a dilute solution, and the salt concentration increased progressively. As seen in the figure, $\Delta\varphi_m$ showed no appreciable change with an increase of the salt concentration and stayed constant (about 17 mV) until C_2 arrived at 1/32 M. The ideal value of the membrane potential for a permselective negative membrane at the concentration ratio of 2.0 is 17 mV. When the concentration C_2 rose to 1/16 M, the observed membrane potential decreased appreciably in a short period of time.

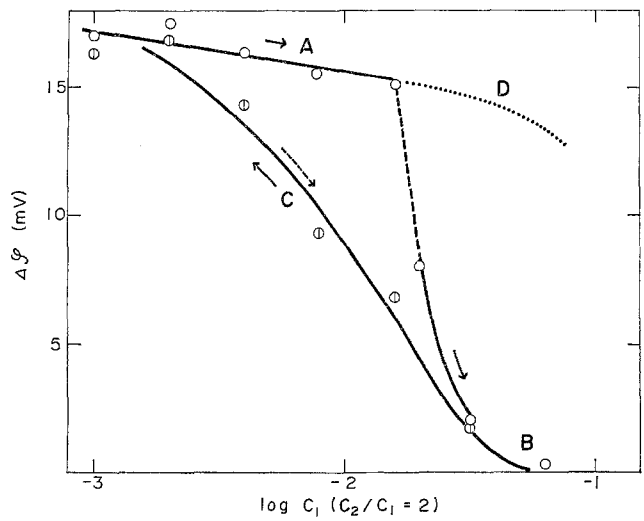

Fig. 7. Membrane potential data $\Delta\varphi_m$ as a function of log C_1 in KCl solution with fixed $\beta = C_2/C_1 = 2.0$ for a membrane with $Q = 2.0$ mg/cm^2. The solid line marked B and C is the theoretical curve of $\Delta\varphi_m$ with a constant effective charge density $\theta = 0.016$ Equiv/liter (*see* refs. [4] and [11])

Further increase of the concentration led to a smooth decrease of the membrane potential as illustrated by mark B in Fig. 7. If the external salt concentration was decreased successively from this stage, $\Delta\varphi_m$ increased smoothly as shown by the arrow marked C in Fig. 7. It was noted that both B and C followed the fixed charge theory of membrane potential. The solid line in Fig. 7 (B and C) shows the theoretical curve with the effective charge density $\theta = 0.016$ Equiv/liter fixed on the membrane [4, 6, 11]. As seen in this figure, the membrane potential observed in the present system indicates a hysteresis loop. When the membrane was in state C, an increase of the salt concentration led to a smooth decrease of $\Delta\varphi_m$ following curve C and B as illustrated by a broken arrow. However, if the membrane was permitted to stand more than several hours in a very dilute salt solution, the membrane returned to state A, and hence $\Delta\varphi_m$ followed a cycle of hysteresis loop of $A \rightarrow B \rightarrow C \rightarrow A \rightarrow$. When the external solutions of 1/1024 and 1/512 M were replaced by a pair of solutions whose concentrations were higher than c_t without successive increase, $\Delta\varphi_m$ fell on the dotted line (marked D) in Fig. 7, although $\Delta\varphi_m$ in this state decreased toward B within a few hours. Both Figs. 6 and 7 show that the observed membrane potential gives two distinct values at the same external salt condition depending upon the history of the membrane.

Four Different States of the Membrane

The simultaneous measurements of the membrane potential and the electric capacitance reveal that states *A* and *C* have roughly the same small value of C_p^0 ($\cong 10^4$ pF/cm^2), while states *B* and *D* have a large C_p^0 ($\cong 10^5$ pF/cm^2). In other words, states *A* and *C* correspond to group *1*, and states *B* and *D* belong to group *2* in Fig. 2. As discussed above, the data of membrane potential, d-c conductance, and ion permeability show that there is no distinction between states *B* and *C*, and also between states *A* and *D*. In state *A*, no permeation of ions was detected, and also no dependence of d-c conductance on the salt concentration was observed. Thus the transport process in state *A* can be concluded to be nonionic, and the observed membrane potential is not a diffusion potential but a phase boundary potential. This conclusion is consistent with the previous argument that group *1* in C_p plots represents an oil membrane, or the DOPH sticks as oil droplets in the filter paper. On the other hand, states *B* and *C* are considered to be a leaky charged membrane, since the concentration dependence of the membrane potential of both *B* and *C* is represented quantitatively by the theory of a constant fixed-charge membrane, and since the ion permeability and d-c conductance are proportional to the concentration of salt in the external solution in these two states. The difference of C_p^0 in states *B* and *C* stems from the difference of the conformation of DOPH in the filter paper, i.e. an oil droplet of DOPH may be changed to a bilayer leaflet with increase of the salt concentration at c_t. The reason that the membrane potentials in *B* and *C* follow the same theoretical curve with a constant fixed-charge density in spite of large difference in C_p^0 in these two states is the physical nature of the membrane potential, i.e. the emf across the membrane is independent of the membrane area. Thus, it is considered that a fraction of the oil membrane in *A* changes its state to a leaky and charged one in *C*, where a number of DOPH bilayer leaflets may be formed in the filter paper; the membrane potential reflects only this part. Similarly, state *D* is continuous with *A* potential-wise, but this state has large C_p^0 in comparison with state *A*. Various properties in different states of the membrane are summarized in Table 1.

It is worthwhile to note that the pH value of the external solution does not affect the impedance behavior of the membrane; i.e., the concentration dependence of C_p is not changed at all because of the variation of pH in the external solution. The membrane potential, on the other hand, decreased with decrease of pH in the solution. At pH = 3.0 in the external solution, the observed membrane potential was diminished in the whole

Table 1. Comparison of some physical properties in four different states of the Millipore-DOPH membrane

State		Electric capacitance C_p^0 (pF/cm^2)	d-c Conductance G_p^0 (mho/cm^2)	Membrane potential $\Delta\varphi_m$	Ion permeability P	Stability
1 ($c_s < c_t$)	A	10^4	independent of c_s 10^{-6}	ideal	non-permeable	stable
	C	10^4	proportional to c_s $>10^{-4}$	leaky charged membrane	permeable	meta stable
2 ($c_s > c_t$)	B	$>10^5$	proportional to c_s $>10^{-4}$	leaky charged membrane	permeable	stable
	D	$>10^5$	independent of c_s 10^{-6}	ideal	non-permeable	meta stable

range of the salt concentration studied. From these results, the state of DOPH in the filter paper is practically determined by the salt concentration in the solution, while the membrane potential is only a reflection of the charged groups bearing on the DOPH molecules.

Stability of Each State of the Membrane

In dilute solutions where both C_1 and C_2 are lower than c_t, the stable state of the Millipore-DOPH membrane is A. The membrane potential in state C increases toward A when the membrane is allowed to stand in this salt condition for several hours. On the other hand, when the concentrations in the external solutions, C_1 and C_2, are higher than c_t, state B is more stable than D. The membrane potential observed in state D tends to decrease toward B within a few hours. These tendencies are observed also for the d-c conductance of the membrane. Under an appropriate salt condition in which the critical concentration c_t is placed between C_1 and C_2, it is possible to make an external condition so that A is stable in comparison with C. In this case, if a pressure difference is applied across the membrane from the concentrated solution to the less concentrated side so that the concentrated solution flows into the membrane, $\Delta\varphi_m$ decreases toward C in a short period of time, but removal of the pressure difference leads a gradual increase of the membrane potential toward A. Fig. 8 illustrates

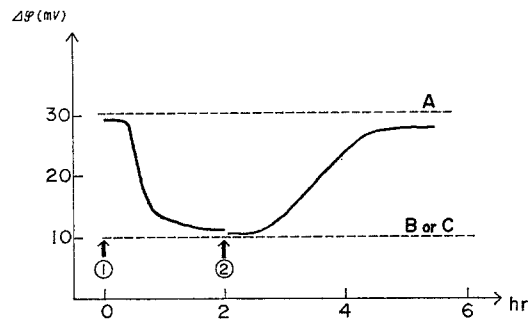

Fig. 8. Variation of $\Delta\varphi_m$ with time, when a pressure difference is applied (mark ①) and released at mark ② from the concentrated solution side for a membrane with $Q=3.10$ mg/cm^2, $C_1=1/128$ M, and $C_2=1/32$ M of NaCl solutions. Broken lines A and B (or C) represent $\Delta\varphi_m$'s for corresponding steady-state values for the present system

the effect of pressure difference applied externally on $\Delta\varphi_m$ for a membrane with $Q=3.10$ mg/cm^2 immersed between 1/128 M and 1/32 M NaCl solutions. Note that a transient variation of $\Delta\varphi_m$ from state B to state D is also possible by an appropriate selection of the external salt concentrations. The variation of the membrane state is also produced by an external electrical stimulus.

Concluding Remarks

Experimental data described in this article can be interpreted at least qualitatively, by the transformation of DOPH in the filter paper from an oil membrane to a charged membrane. However, the final justification on this view is left for future works with which the presence of two conformational states of DOPH in the filter paper should be detected by a direct means.

As shown in the text, the membrane potential observed in the present system has two distinct values with a given set of external salt conditions according to the history of the membrane. These two states may be interchangable by external stimuli applied across the membrane. Hence, the present membrane may be used as a model system for excitable living membranes or receptor cells. Further studies will appear in a subsequent article of this series.

This work was supported in part by the grant-in-aid for the special project in biophysics from the Ministry of Education, Japan, and also by the Takeda Science Foundation.

References

1. Cohen, L. B., Keynes, R. D., Hille, B. 1968. Light scattering and birefringence changes during nerve activity. *Nature* **218**:438.
2. Howarth, J. V., Keynes, R. D., Ritchie, J. M. 1968. The origin of the initial heat associated with a single impulse in mammalian non-myelinated nerve fibers. *J. Physiol.* **194**:745.
3. Leninger, A. L. 1968. The neuronal membrane. *Proc. Nat. Acad. Sci.* **60**:1069.
4. Kamo, N., Toyoshima, Y., Kobatake, Y. 1971. Fixed charge density effective to membrane phenomena, Part I. Mobilities and activity coefficients of small ions in charged membranes. *Kolloid Z.* **248**:914.
5. Kobatake, Y., Irimajiri, A., Matsumoto, N. 1970. Studies of electric capacitance of membranes. I. A model membrane composed of filter paper and lipid analogue. *Biophys. J.* **10**:728.
6. Kobatake, Y., Takeguchi, N., Toyoshima, Y., Fujita, H. 1965. Studies of membrane phenomena. I. Membrane potential. *J. Phys. Chem.* **69**:3981.
7. Kobatake, Y., Tasaki, I., Watanabe, A. 1971. Phase transition in membrane with reference to nerve excitation. *Advanc. Biophys.* **2**:1.
8. Singer, I., Tasaki, I. 1968. Nerve excitability and membrane macromolecules. *In:* Biological Membranes. D. Chapman, editor. Ch. 8, p. 347. Academic Press Inc., New York.
9. Tasaki, I. 1968. Nerve Excitation. Charles C. Thomas, Springfield, Ill.
10. Tobias, J. M., Agin, D. P., Pawlowski, R. 1962. Phospholipid-cholesterol membrane model: Control of resistance by ions or current flow. *J. Gen. Physiol.* **45**:989.
11. Toyoshima, Y., Kobatake, Y., Fujita, H. 1967. Studies of membrane phenomena. IV. Membrane potential and ion permeability. *Trans. Faraday Soc.* **63**:2814.
12. Yoshida, M., Kobatake, Y., Hashimoto, M., Morita, S. 1971. Studies of electric capacitance of membranes. II. Conformational change in a model membrane composed of a filter paper and a lipid analogue. *J. Membrane Biol.* **5**:185.